Impacts of Summer Monsoons on Flood Characteristics in the Lancang-Mekong River Basin

Jie Wang[1,2], Qiuhong Tang[1,2], Aifang Chen[3], Yin Tang[1], Ximeng Xu[1], Xiaobo Yun[1,2], Mengfei Mu[1], Nigel Wright[4], Deliang Chen[5]

[1]*Key Laboratory of Water Cycle and Related Land Surface Processes, Institute of Geographic Sciences and Natural Resources Research, Chinese Academy of Sciences, Beijing, China*

[2]*University of Chinese Academy of Sciences, Beijing, China*

[3]*School of Environmental Science and Engineering, Southern University of Science and Technology, Shenzhen, China*

[4]*School of Architecture, Design and Built Environment, Nottingham Trent University, NG1 4FQ Nottingham, UK*

[5]*Regional Climate Group, Department of Earth Sciences, University of Gothenburg, Gothenburg, Sweden*

Correspondence to: Qiuhong Tang, tangqh@igsnrr.ac.cn

Highlights:

- The impacts of monsoon on flood characteristics were assessed at local and spatial scales.
- Flood start date advances, Q_{10} and flood volume increase during the strong monsoon years.
- Monsoon impact on flood is regionally distributed with impact in tributary larger than mainstream.
- The trade-off of water from different areas can disturb the tendency of monsoon impact on flood.

Abstract

The impact of monsoon on rainfall in the Lancang-Mekong River Basin (LMRB) has been well understood, but its impact on flood characteristic across the basin is still unclear. To investigate this impact, the Variable Infiltration Capacity (VIC) hydrological model was used to generate the basin-wide discharge and extract flood characteristics. Indian Summer Monsoon (ISM), Western North Pacific Monsoon (WNPM), and their combined effect (ISWN) were considered and represented by monsoon index. The monsoon impact area was firstly obtained based on the monsoon impact on rainfall, followed by the anomaly analyses of flood characteristics within the impact area to quantify the monsoon impact on floods at local and spatial scales. The results show that the ISM and WNPM (or ISWN) can significantly modulate up to 20% of the rainfall interannual variability in the western and eastern parts of the basin, respectively. The monsoon impact on flood is regionally distributed with impact in tributary larger than mainstream. Over half of the monsoon impact areas show the flood start date averagely advances (delays) 8–12 days, flood volume averagely increases (decreases) by 9%–17.5% and Q_{10} averagely increases (decreases) by 7.4%–14.4% during the strong (weak) monsoon years. Also, the comparisons between monsoon local and spatial impacts reveal that the trade-off of water from different areas can disturb the monsoon impact on flood, suggesting that more stations should be used when using the observed data to analyze the monsoon impact. More importantly, the ISM tends to cause the severe flood in northern Thailand, while WNPM and ISWN mainly induce the severe flood in the southeastern part of the

LMRB. This study could help to increase the knowledge of the impact of climate change on flood and help with the regional flood managements.

Key words: Flood Characteristics, Indian Summer Monsoon, Western North Pacific Monsoon, VIC model, Lancang-Mekong River Basin

1. Introduction

Water related disasters account for about 90% of the world's natural disasters, causing more than 45% of the total human live loses and 90% of the affected population in Asia (*Adikari and Yoshitani*, 2009). Flood, in particular, contributes to more than 43% of the total occurrence of natural disasters (*Wahlstrom and Guha-Sapir*, 2015; *EM-DAT*, 2019). This disaster frequently occurs in the low-lying areas where the rivers are widely developed and population is highly concentrated (*Wang et al.*, 2019). However, due to the lack of the effective flood monitoring and forecasting, the occurred flood could frequently cause casualties and property damages (*Wu et al.*, 2014), especially in the less developed areas and countries. More importantly, many evidences have shown the increasing flood around the world (e.g., *Petrow and Merz*, 2009; *Hirsch and Archfield*, 2015), which is likely to continue in the future under the background of climate change (e.g., *Hirabayashi et al.*, 2013; *Hoang et al.*, 2016; *Wang et al.*, 2017). This will potentially cause the increasing economic losses (*Bouwer*, 2011; *Dottori et al.*, 2018), and have attracted worldwide concern (*Zhang et al.*, 2018). World Water Development Report 4 has pointed out that about 2 billion populations will be suffered from flood disaster by 2050 (*UNESCO*, 2012), where one of the causes is climate change. Thus, understanding the impact of climate change on flood is crucial to flood risk management.

The Langcang-Mekong river, having a total length of 4,800 km (*MRC*, 2006), originates from the Tibetan Plateau, runs through China, Myanmar, Laos, Thailand, Cambodia, Vietnam, and ends in the South China Sea (Figure 1). Since most of the lower Mekong river basin (MRB) is plain or delta, added by highly concentrated population and less developed economy, this area is a flood-prone zone with the world highest flood-induced mortalities (*MRC*, 2015; *Hu et al*., 2018; *Chen et al*., 2020). A broad estimate of up to 76 million US dollars average annual damage has been caused by floods, which can rise to over 800 million US dollars in an extreme year such as 2000 (*MRC*, 2009). In the past decades, this basin has experienced climate change (e.g., changing monsoon) and intensified anthropogenic activities (e.g., dam construction, irrigation expansion) (e.g., *Hossain et al*., 2017; *Hoang et al*., 2019; *Tang*, 2020; *Triet et al*., 2020), leading to these two factors are two major hydrological issues in this basin (e.g., *Wang et al*., 2017; *Pokhrel et al*., 2018). Particularly, the climate change is expected to continue and will exacerbate the flood risk (e.g., *Wang et al*., 2017; *Triet et al*., 2020), making this factor become one of the most important sources in affecting the flood in this basin. A study based on the climate projections has reported that up to 140% and 55% flood frequency and magnitude increasing rate might be introduced in future (*Wang et al*., 2017). It is necessary to understand how climate change affects the flood in this basin.

In the LMRB, the sources of flood are mainly from monsoon rainfall, the snowmelt from Tibetan Plateau, and localized tropical storms (*Delgado et al*., 2012). The monsoon rainfall, lasting from May until September or early October (*MRC*, 2006), contributes to 80%–90% of the discharge for the lower Mekong River, and is a major factor of flood occurrence (*Delgado, et al*., 2012; *Lauri, et al*., 2012). Two monsoon systems, namely the Indian Summer Monsoon (ISM) and Western North Pacific

Monsoon (WNPM), regulate this monsoon rainfall, and make the rainy season rainfall account for 80% of its annual precipitation (*Yang et al.*, 2019). Therefore, understanding the monsoon impact on flood is an important link for the knowledge of the impact of climate change on flood.

Usually, the monsoon takes effects on flood mainly through rainfall. Many valuable studies have been carried out for the impact of monsoon on rainfall. For example, *Yang et al.* (2019) studied the relationship between rainfall anomaly and the covariability of ISM and WNPM (i.e., monsoon combined effect). They found the rainfall in the LMRB was significantly regulated by the covariability. When ISM and WNPM is higher (lower) than normal, then the combined effect is higher (lower) than normal, and therefore the rainy rainfall mainly presents the positive precipitation in the LMRB. Also, their results indicated that the ISM mainly affects the rainy season rainfall west of the LMRB, while WNPM affects the southeastern LMRB. The monsoon rainfall anomaly is more (less) when ISM or WNPM is strong (weak), and vice versa. This positive correlation was also detected by *Fan and Luo* (2019), where over 29.3% and 12.8% of the basins showed this pattern with respects to WNPM and ISM, respectively.

In addition to the researches related to the monsoon impact on rainfall, a few studies have also turned their views on monsoon impact on flood. *Delgado et al.* (2012) found a positive correction between WNPM and the average discharges from June to November at Kratie and other stations in the lower MRB, while ISM had less impact on these selected stations. Similar finding was also obtained by *Fan and Luo*

(2019). These works provide valuable information for our understanding about monsoon impact on flood. However, their analyses were mainly based on the several stations on the river mainstream. Some information could be lost due to the limited number of stations (e.g., the ISM impact on flood). More importantly, the river mainstream receives water not only from the local but also from the upstream, where monsoon in these areas can have less impact on rainfall or show different pattern with rainfall (e.g., *Delgado, et al.*, 2012; *Fan and Luo* 2019; *Yang et al.*, 2019). This could lead to the uncertainty in analyzing the monsoon impact on flood if only the limited stations were used. Extending the monsoon impact on flood at local scale to spatial scale is very important to understand the monsoon impact on flood deeply.

In this paper, we intended to investigate the monsoon spatial impacts on flood, following the monsoon impact on flood at stations (i.e., monsoon local impacts). The spatially distributed flood characteristics were obtained using the Variable Infiltration Capacity (VIC) hydrological model. Two monsoons (i.e., ISM and WNPM) and their combined effect (donated as ISWN, assuming to be a monsoon for an easier description) were all considered, where their interannual variabilities in the monsoon strength were derived from the monsoon indices. Thus, the linkage between monsoon and basin wide flood can be assessed by anomalies in the strong and weak monsoon years. These analyses can help increase our knowledge of the monsoon impacts on flood in the LMRB, and can also be extended to other basins affected by monsoon.

2. Data and Methods

2.1 Model description

Hydrological model is an effective tool to understand and quantify the behavior of the water cycle and its components (e.g., *Deb et al*., 2019; 2020). In this research, the VIC model (*Liang et al*., 1994, 1996) with the river routing model (*Lohmann et al*., 1996) was adopted to simulate the discharge in the LMRB, where satisfactory model performance has been achieved in previous studies (e.g., *Hossain et al*., 2017; *Yun et al*., 2020). This model is a grid-based model and considers snowmelt and frozen soil physical processes, and calculates energy and water budgets for each grid at daily or sub-daily time step, with topography and vegetation presented at sub-grid scale. The river routing model routes the runoff produced by VIC to the outlets using the unit-hydrograph (UH).

Large-scale effects due to summer monsoons, added by the spatial resolution of the available meteorological inputs, the spatial resolution for VIC model was set to 0.25°×0.25°. Both the meteorological data to run the model and discharge data to calibrate and validate the model were collected separately for Lancang River Basin and Mekong River Basin (see Table 1 for details). The spin-up period was considered as 1961–1966, and repeated twice to provide a relatively steady initial state, while calibration and validation periods were determined to be 1967–1991 and 1992–2007 respectively. Data after 2007 were not used for calibration and validation mainly because many dams were constructed and operated during the last decade and 1.7% of the Mekong mean annual discharge has been impacted by dams until 2007 (*Kummu et al*., 2010; *Hecht et al*., 2019).

2.2 Flood characteristics

Similar to *Räsänen and Kummu* (2013), five flood characteristics including start date (onset, *O*), end date (termination, *T*), duration (*D*), peak (*P*), and volume (*V*) were selected to represent the seasonal flood characteristics. Considering that the discharge hydrograph during a typical year usually has only one up-crossing and single down-crossing sections (*MRC*, 2007), the long-term annual average (i.e., Q_{50}) to split the hydrograph used by *MRC* (2007) was adopted in this research to obtain the flood parameters. The start date was defined as the date when the daily discharge started to exceed the annual average, while the end date was the date when the daily discharge started to fall below the average. The flood duration was defined as the interval between the start date and end date, while the flood volume was the accumulated water volume on the days during the flood duration. The flood peak was defined as the maximum daily discharge during the selected calendar year (diagram see *Räsänen and Kummu* (2013)). Instead of choosing a steady relative long up (or down) period to determine the flood start and end dates (*MRC*, 2007; *Räsänen and Kummu*, 2013), moving average method was used to minimize the simulated discharge oscillation impacts caused by the uncertainty in meteorological inputs, i.e., increasing the moving average length from 3 days to the days when there existed at most 4 intersection points between the annual average and final moving average line. Then the dates, expressed as the day of year, separately corresponding to the first and last points, were selected as the flood start date and end date. In addition, referring to

Kiem et al. (2008), Q_{10} was also used to represent the flood extreme, which sorted the discharge series of a given year in a descending order and taken 10% percentile. Indicators including Nash-Sutcliffe efficiency (*NSE*), Person correlation coefficient (*R*) were used to quantitatively assess these extracted flood characteristics (detailed formulas see *Gupta et al*., 2009; *Wang et al*., 2016; *Zhao et al*., 2019).

2.3 Monsoon index

As the monsoon systems influence the LMRB mainly from June to September, the mean monsoon index defined by *Wang et al.* (2001) from June to September was used to represent the summer monsoon intensity of this year. Accordingly, the accumulated rainfall from June to September was used as the rainy season precipitation (*Yang et al*., 2019). Considering the fundamental driver of LMRB hydro-climate is the combined ISM and WNPM (e.g., *Delgado et al*., 2012), a synthetic monsoon index defined by *Yang et al*. (2019) (i.e., ISM index plus WNPM index with the same weight) was adopted to reflect the covariability of the ISM and WNPM (i.e., the combined effect ISWN). These three monsoon indices were normalized during 1967–2015, with the normalized value larger than 1 and less than -1 separately representing the strong and weak monsoon (Figure 2). Consequently, the normalized monsoon index ranging from -1 to 1 represented the normal monsoon. Similar approach was also employed in *Li et al*. (2016) and *Yang et al*. (2019). Here, the combined effect ISWN was assumed to be also a monsoon for easier description and comparison.

2.4 Monsoon impact on flood

The basic flowchart to conduct monsoon impact on flood is illustrated in Figure 3. The anomaly, defined as the average deviation relative to the average value of normal monsoon years, was used to quantify the flood change during the strong or weak monsoon years. Considering the discharge is the superimposition of the runoff from different location and time, which may be distributed by the runoff from area with less affected by monsoon, the Person correlation coefficient (R) was used to identify the area affected by monsoon. Here, based on the positive relation between the monsoon and rainfall that has been found by *Yang et al.* (2019) and *Fan and Luo* (2019), the area with positive correlation between monsoon index and rainy season rainfall (i.e., rainfall increases when monsoon strengthens, and it decreases when monsoon weakens) was identified as the area affected by monsoon (i.e., monsoon impact area). In this way, the maximum area with monsoon impact on rainfall was detected, and the analyses for monsoon impact on flood could be limited to the spatial extent where monsoon takes effect on rainfall. Three representative stations Chiang Sean (CS), Pakse (PK), and Stung Treng (ST), located in different monsoon impact areas, were selected to analysis the monsoon local impact and make comparisons with the monsoon spatial impact. In addition, to make a clearer distinguishment for monsoon spatial impact on flood, the anomalies across the basin were re-interpolate to 500 meters using the inverse distance weighted method, which could have less impact on the results.

3. Results

3.1 Monsoon impact areas

Figure 4 shows the spatial distributions of the rainfall anomalies in the weak and strong monsoon years, where the area affected by monsoon was also delineated (Figures 4a-c). The positive impact of monsoon on rainfall can be found in most areas of the MRB, especially for ISM and ISWN. This agrees with *Yang et al*. (2019) and *Fan and Luo* (2019). For ISM, the affected area is mainly located in the western part of the MRB. For WNPM, the affected area is mainly located in the eastern and parts of the MRB and downstream of the Lancang River Basin. The area affected by ISWN covers most of the areas affected by WNPM and is extended to the areas that are affected by ISM. Similar distributions for affected area can also be found in *Delgado et al*. (2012) and *Yang et al*. (2019). Note that some areas, such as the downstream of the Lancang River Basin and northern Thailand, individually affected by ISM or WNPM are diminished when affected by ISWN. This potentially indicates the coexistence of monsoon impacts across the basin, where strong ISWN is usually with strong ISM or WNPM (Figure 2).

Further, the areas affected by ISM, WNPM and ISWN account for 42.7% (51.3%), 29.0% (28.6%), 44.9% (55.6%) of the total LMRB (MRB) area, respectively. These values are different with the results of *Fan and Luo* (2019), where they analyzed the area significant affected by monsoon and different precipitation dataset was used. Nevertheless, it reveals the dominant roles of the ISM and ISWN on rainfall in the spatial impact distribution. Moreover, the increase (decrease) in rainfall can reach over 20% in the strong (weak) monsoon years. Note the disagreement between rainfall anomaly and monsoon change in the upstream of the Lancang River Basin, which may be related to the topography (see *Delgado et al.*, 2012).

3.2 Model performances

The flood characteristics (i.e., start date, end date, duration, peak, volume and Q_{10}) were extracted from both the simulated and observed discharge hydrographs, and the results are shown in Figure 5. It can be found that the simulated characteristics are close to those of the observation, confirming that the VIC simulation is capable of flood characteristic extraction. For each characteristic at each considered station, the R and NSE are large than 0.66 and 0.12, respectively. The performances at stations in the upstream (i.e., CS and PK) tend to be better than downstream (i.e., ST). Also, the flood volume and Q_{10} are generally better simulated than other flood characteristics at each station. More importantly, the simulation in tendency (R) is better than magnitude (NSE), indicating the anomaly signal can be greatly preserved while its magnitude could be affected.

3.3 Monsoon local impacts on flood

The impacts of monsoon on flood characteristics at three representative stations (i.e., CS, PK and ST) are shown in Figure 6. The anomalies of the simulated value fundamentally reflect the changes of the observation, though the magnitudes in most cases are underestimated. At CS station, located in the ISM impact area, the flood start date advances (delays), Q_{10} decreases (increases) when ISM is strong (weak). Whether ISM is strong or weak, the end date delays and flood peak decreases (Figure 6a). Each characteristic has an anomaly within the range from -9% to 7%.

At PK station, located in the area affected by WNPM and ISWN, the results reveal that the flood start date advances (delays), volume and Q_{10} increase (decrease) when WNPM strengthens (weakens) (Figure 6e). All flood characteristics change from -14% to 16% during the strong and weak WNPM years. Similar results can be found for ISWN (Figure 6f). Here, each flood characteristic changes within the range of -21%–11% during the strong and weak ISWN years.

At ST station, located in the area mainly controlled by ISM and ISWN, the flood start date advances, peak, volume and Q_{10} increase when ISM is strong (Figure 6g). When ISM is weak, the peak and Q_{10} still increase, while flood end date delays and flood duration decreases. The flood characteristic anomalies are in a range from -3% to 11% during the anomalistic ISM years (i.e., strong and weak ISM years). When ISWN strengthens (weakens), the flood start date advances (delays), all duration, peak, volume, Q_{10} increase (decrease) (Figure 6i). The anomalies of flood characteristic during the ISWN anomalistic years is from -26% to 17%.

3.4 Monsoon spatial impacts on flood

Figure 7 shows the spatial distributions of the flood characteristic anomaly that consider two strong and weak ISMs. Regionally distributed affected area can be found with different trend (positive or negative). When ISM is strong, the maximum anomaly values for flood volumes mainly occur in northern Thailand (adjacent to the northeastern Myanmar and northern Laos; Figure 7i), which is consistent with the rainfall anomaly (Figure 4a). In this area, over 15% of the rainfall anomaly is found due to the close distance to the Bay of Bengal, and therefore it can cause more severe flood (i.e., larger flood volume anomaly). Further, in ISM impact area, the strong ISM mainly makes the flood start date averagely advance 8 days (4.4% for anomaly, same as bellow), end date averagely delays 5 days (1.7%), and flood peak, volume, Q_{10} and duration averagely increase by 12.1%, 11.5%, 9.3% and 7.1%, respectively (Figures 7a-d, i, k). At least 59.7% of the ISM impact area shows the above impacts. Particularly, over 80% of the ISM impact area occurs the increasing flood volume and Q_{10} in the strong ISM years. When ISM is weak, over 70% of the ISM impact area reveals the delayed flood start date, advanced end date, decreased flood duration, flood peak, Q_{10} and flood volume (Figures 7e-h, j, l). On average, the flood start date delays 12 days (7.2%), the end date advances 9 days (2.8%), and flood duration, peak, volume, and Q_{10} decrease by 12.5%, 15.8% and 17.5%, -14.4%, respectively. It is worthy to note that over 87% of the ISM impact area shows the reduced flood peak, flood volume, and Q_{10}.

The spatial impacts of WNPM on flood characteristics are illustrated in Figure 8. The results show that the area prone to high flood volume and Q_{10} during the strong WNPM years is in the “3S” river basin (i.e., Sekong, Se San, Sre Pok; Figures 8i, k), with the largest rainfall amount anomaly (Figure 4b). When WNPM is strong, over

57% of the WNPM impact area has the tendency of advancing the flood start date and end date, decreasing the flood peak, and increasing the flood volume, Q_{10}, flood duration (Figures 8a-c, i, k). On average, the flood start date and end date in these regions separately advances 11 days (6.2%) and 4 days (1.3%), the flood volume, duration and Q_{10} increase by 10.4%, 8.7%, 7.4%, respectively. However, the flood peak averagely reduces by 8.0% in these regions, different from the flood volume and Q_{10} (Figures 8d, i, k). This is especially obvious for flood peak in the central Laos, where the rainfall amount, flood volume and Q_{10} increases (Figures 4b, 8d, i, k). The main reason is the underestimation of heavy rainfall that determines the flood peak, and can be inferred from Figure 4 in *Lauri et al.* (2014), where the annual precipitation of APHRODITE seems to be underestimated when compared with the observation data. During the weak WNPM years, over 50% of the WNPM impact area shows the delayed flood start date and end date, reduced flood peak, volume and Q_{10}, and increased flood duration (Figures 8e-h, j, l). On average, the flood start date in these areas delays 8 days (4.6%), end date delays 11 days (3.6%), flood duration increases by 8.2%, and flood peak, volume and Q_{10} decrease by 10.1%, 9.0% and 10%, respectively.

The ISWN spatial impacts on flood are shown in Figure 9. The results show that the maximum anomalies during the strong ISWN years for flood peak, flood volume and Q_{10} mainly occur in the “3S” river basin (Figures 9d, i, k), where more than 20% anomaly of rainfall occurs in this area (Figure 4c). This indicates that more severe flood with higher flood peak or larger flood volume can occur in the "3S" river basin easily. During the strong ISWN years, over 60% of ISWN impact area occurs with the advanced flood start date, delayed flood end date, and increased flood duration, volume, Q_{10} and peak (Figure 9a-d, i, k). On average, the flood start date in these regions advances 8 days (4.6%), flood end date delays 4 days (1.4%), and the flood duration, peak, volume and Q_{10} increase by 8.3%, 10.3%, 14.3% and 12.5%, respectively. Particularly, more than 90% of the ISWN impact area shows the increased flood volume and Q_{10}. In weak ISWN years, over 66% of ISWN impact area shows the flood start date delays 10 days (6.1%), flood end date delays 5 days (1.6%), and flood duration, volume, peak, and Q_{10} reduce by 6.7%, 12.8%, 14.4% and 12%, respectively (Figures 9e-h, j, l).

4. Discussion

4.1 Monsoon impact comparisons

Usually, when monsoon is strong, then the rainfall amount should be larger than normal condition (e.g., *Yang et al.,* 2019), and the discharge rises earlier and drops later, thus causing the longer flood duration and larger flood volume. Under this condition, the soil can be saturated earlier and thus making the flood peak much higher. Similar results can be inferred for weak monsoon. Consequently, in a typical year, the ideal results for monsoon impact on flood are the flood start date advances (delays), end date delays (advances), and flood peak, volume, Q_{10}, duration increase (decrease) during the strong (weak) monsoon years. The mostly consistent results are found for ISM spatial impacts on flood (Figure 7). However, different results for monsoon impact of ISM are found at CS station (Figure 6a). It is found that flood peak decreases and flood end date delays whether ISM is strong or weak. The reason causing this difference is the spatial location where the results are analyzed. The CS station is located on the mainstream of Mekong River, while the areas showing the general monsoon spatial impact on flood are located in the upstream (i.e., tributary) of the mainstream (i.e., downstream). The CS station receives water not only from the ISM impact area, but also from the mainstem upstream of it that is not affected by ISM (Figure 4d). The trade-off between both sides disturbs the trend of the ISM impact on flood at CS station, indicating the uncertainty in analyzing the impact of monsoon on flood exists if only several stations are considered, especially for the stations on the mainstream.

Nevertheless, the impacts of WNPM and ISWN on most of the flood characteristics are consistent between local and spatial scales (Figure 6, 8, 9), which also agree well with the ideal results. The reason for this is the close distance of the selected stations (i.e., PK and ST) to the downstream of the impact area, where the monsoon in this impact area primarily dominates the hydrology regime when compared to the impact of upstream water affected by other type of monsoon or less affected by monsoon. This highlights the importance of the location for the station used for analyses when related to the impact of monsoon on flood, suggesting that more stations should be considered when analyzing the impact of monsoon on flood if only observations are used.

Also, the basically identical results are found for WNPM and ISWN impacts on flood characteristics at PK station (Figure 6e, f). However, inconsistent results occur for ISM and ISWN impacts at ST station (Figure 6g, i). For example, it was found the flood peak at ST station increases whether ISM is strong or weak. The reason for this may be related to the smaller contribution of ISM impact area around ST in affecting flood, making the ISM impact here is negligible (also see *Delgado et al*., 2012). Consequently, the impact of ISM at this station is not the true impact of ISM. Noting that some stations like CS station are not in the areas affected by ISWN, potentially demonstrating the spatial coexistence of the monsoon impacts on flood.

Comparing with the inconsistences of different monsoon impact existing at the local scale (i.e., station), more identical results are found for different monsoon spatial impacts on flood characteristics. It is found the monsoon spatial impact on flood on tributary is likely to be larger than that on mainstream, and such impact is regionally distributed. The flood start date averagely advances 8–11 days (i.e., changing from -4.4% to -6.2%), flood volume increases by 10.4%–14.3%, Q_{10} increases by 7.4%–12.5%, and flood duration increases by 7.1%–8.7% over half of the monsoon impact area during the strong monsoon years. During the weak monsoon years, over half of the monsoon area shows that the flood start date averagely delays 8-12 days (4.6%–7.2%), flood volume averagely decreases by 9%–17.5%, Q_{10} decreases by 10%–14.4%, and flood peak also reduces by 10.1%–15.8%. These results are consistent with ideal results, potentially indicating the reasonability of our analyses for the mechanism of the monsoon impact on flood. However, the differences among three monsoons for their spatial impacts on flood characteristics also exist. For example, whether WNPM is strong or weak, flood duration increases and flood peak reduces. This is different from those of ISM or ISWN, where flood duration and flood peak increase (decrease) when ISM or ISWN is strong (weak). The reason causing the longer flood duration in weak WNPM years and smaller flood peak in strong WNPM years might be the underestimation of heavy rainfall as shown above. The underestimation of heavy rainfall could lead to the underestimation of flood peak and long-term average discharge to split the hydrograph, and therefore causing the longer flood duration. In addition, affected by the interaction between the ISM and WNPM, the tendency for ISWN impact on flood is either same with ISM or same with WNPM.

4.2 Uncertainties and limitations

There are several uncertainties and limitations related to this research. Firstly, due to the relatively scarce available observed meteorological data in the LMRB (e.g., *Yatagai*, *et al*., *Lauri et al*., 2012, 2014), the gridded data rather than in-situ data were collected for Lancang River basin and MRB, respectively. These gridded data were interpolated at spatial and temporal scales using in-situ data. Therefore, the accuracy of the gridded product is limited due to the coarse station network density and uneven station distribution (*Wang et al*., 2016), especially for precipitation which has a critical role in runoff (*Liu et al.*, 2018) and thus in flood performance. This may have an impact on the model performance in flood simulation. To reduce the precipitation uncertainty impact, the precipitation dataset APHRODITE was selected, which has been proved to be one of the best precipitation datasets in MRB hydrological application (*Lauri et al*., 2014; *Tian et al*., 2021) and was used as a reference for other precipitation dataset comparisons (*Chen et al*., 2018). However, the storm causing the big flood is local but with extremely large value, which is hard to capture and is easily picked out as an outlier. Consequently, the interpolated precipitation could largely underestimate the heavy storm that determines flood, especially for flood peak. These can be inferred from Figure 6 and Figure 8, where the anomaly from simulation is underestimated and flood peak decreases during the strong monsoon years. Therefore, the quality in precipitation is worthy to be further investigated, especially for flood season.

Secondly, the model structure is also an uncertainty source and limitation. In the lower MRB, the controlling factor of water flow is no longer the elevation of ground; instead, the water flow itself may play a key role due to the relative flat topography. The backwater water effect can frequently occur in this area during the flood season, which forms the famous inverse river (i.e., Tonle Sap River; *Hecht et al*., 2019). The flow routing method used in this research is unit hydrograph (*Lohmann et al*., 1996), which can be no longer applied to the flood plain, thus potentially causing the uncertainties. Nevertheless, the method to reflect the impact of monsoon on flood is anomaly, the relative value rather than the absolute value, which can basically preserve the consistency in trend. The hydrodynamic model that can quantify the backwater effect should be considered in future to decrease the uncertainty.

Thirdly, the complex monsoon systems and runoff routing also make the results uncertain and limited. A spatial location can receive water not only from different monsoon types due to the unregular impact area and complex runoff route lines but also from area that is less affected by monsoon. Therefore, the final results could be the trade-off between upstream water and local water, which increases the uncertainty and limitation in analyzing the monsoon impact on flood, especially for the monsoon local impact using the in-situ observations (e.g., on the mainstream). In this research, to decrease the uncertainty caused by complex monsoon systems and runoff routing, analyses were limited to the monsoon impact area to reduce the disturbance from the areas less affected by monsoon. However, the general pattern for monsoon impact on flood characteristics was not fully obtained within the monsoon impact area, such as flood end date, flood duration and flood peak. New methodologies may be needed in future to further improve the results of monsoon impact on flood.

5. Conclusions

This research investigated the monsoon impacts on flood characteristics in the LMRB using the anomaly. Two monsoons (i.e., ISM and WNPM) and their combined effect ISWN were considered and represented by monsoon index. The VIC model with the river routing model was used to generate discharge, from which the flood characteristics including start date, end date, duration, peak, Q_{10} and volume were extracted and validated. The monsoon effects on these flood characteristics were analyzed at local and spatial scales, followed by the discussion of the monsoon impact comparisons.

The ISM dominates the rainfall in the western part of the MRB, while WNPM controls that in the east, and ISWN covers most areas that are affected by WNPM. More importantly, these effects on rainfall can coexist in the basin. When any of them strengths (weakens), up to 20% increase (decrease) in rainfall can occur in the basin, especially for northern Thailand (ISM) and "3S" river basin (WNPM, ISWN) with the maximum increase.

Six selected flood characteristics including flood start date, end date, duration for observation were simulated reasonably well in tendency. At least 0.66 correlation coefficient was obtained for each characteristic at any of three selected stations. Further, the anomalies of the simulated value can fundamentally reflect the changes of the observation, though the magnitudes in most cases are underestimated.

The spatial impact of monsoon on flood is regionally distributed with impact in tributary tending to be larger than mainstream. The general impact of monsoon on flood is that the flood start date averagely advances (delays) 8–12 days, volume averagely increases (decreases) 9%–17.5%, Q_{10} averagely increases (decreases) 7.4%–14.4% over half of the monsoon impact area during the strong (weak) monsoon years. When the monsoon is strong, the flood duration averagely increases by 7.1%–8.7% over half of the monsoon impact area; while the flood peak reduces by 10.1%–15.8% over half of the monsoon impact area during the weak monsoon years.

Except for ISM, the monsoon impacts on flood characteristics are mostly consistent between the local and spatial scales. The inconsistency in monsoon impacts on flood indicates that the monsoon impact on flood characteristics could be disturbed by the trade-off of water from different monsoon impact areas or areas less affected by monsoon. This suggests that more stations should be used when using the observed data to analyze the monsoon impacts on flood.

Acknowledgements

This research was supported by the Strategic Priority Research Program of Chinese Academy of Sciences (XDA20060402), National Natural Science Foundation of China (41730645), the International Partnership Program of Chinese Academy of Sciences (131A11KYSB20180034) and Newton Advanced Fellowship. The monsoon data is obtained from http://apdrc.soest.hawaii.edu/projects/monsoon/.

Reference:

Adikari, Y., Yoshitani, J., 2009. Global trends in water-related disasters: an insight for policymakers. World Water Assessment Programme Side Publication Series, Insights. The United Nations, UNESCO. International Centre for Water Hazard and Risk Management (ICHARM).

Bouwer, L.M., 2011. Have disaster losses increased due to anthropogenic climate change? B. Am. Meteorol. Soc. 92(1), 39-46.

Chen, A., Chen, D., Azorin-Molina, C., 2018. Assessing reliability of precipitation data over the Mekong River Basin: A comparison of ground-based, satellite, and reanalysis datasets. Int. J. Climatol. 38(11), 4314-4334.

Chen, A., Giese, M., Chen, D., 2020. Flood impact on Mainland Southeast Asia between 1985 and 2018-The role of tropical cyclones. J. Flood Risk Manag. 13(2), e12598.

Deb, P., Kiem, A. S., & Willgoose, G. (2019). A linked surface water-groundwater modelling approach to more realistically simulate rainfall-runoff non-stationarity in semi-arid regions. Journal of Hydrology, 575, 273-291.

Deb, P., & Kiem, A. S. (2020). Evaluation of rainfall–runoff model performance under non-stationary hydroclimatic conditions. Hydrological Sciences Journal, 65(10), 1667-1684.

Delgado, J. M., Apel, H., Merz, B., 2010. Flood trends and variability in the Mekong river. Hydrol. Earth Syst. Sc. 14(3), 407-418.

Delgado, J.M., Merz, B., Apel, H., 2012. A climate-flood link for the lower Mekong River. Hydrol. Earth Syst. Sc. 16(5), 1533-1541.

Dottori, F., Szewczyk, W., Ciscar, J. C., Zhao, F., Alfieri, L., Hirabayashi, Y., Feyen, L., 2018. Increased human and economic losses from river flooding with anthropogenic warming. Nature Clim. Change 8(9), 781-786.

EM-DAT, 2019. The Emergency Events Database-Université catholique de Louvain (UCL) CRED, D. Guha-Sapir-www.emdat.be, Brussels, Belgium.

Fan, X., & Luo, X. (2019). Precipitation and Flow Variations in the Lancang–Mekong River Basin and the Implications of Monsoon Fluctuation and Regional Topography. Water, 11(10), 2086.

Gupta, H.V., Kling, H., Yilmaz, K.K., Martinez, G.F., 2009. Decomposition of the mean squared error and NSE performance criteria: Implications for improving hydrological modeling. J. Hydrol. 377(1-2), 80-91.

Hecht, J.S., Lacombe, G., Arias, M.E., Dang, T.D., Piman, T., 2019. Hydropower dams of the Mekong River basin: A review of their hydrological impacts. J. Hydrol. 568, 285-300.

Henck, A.C., Huntington, K.W., Stone, J.O., Montgomery, D.R., Hallet, B., 2011. Spatial controls on erosion in the Three Rivers Region, southeastern Tibet and southwestern China. Earth Planet. Sc. Lett. 303(1-2), 71-83.

Hirabayashi, Y., Mahendran, R., Koirala, S., Konoshima, L., Yamazaki, D., Watanabe, S., ... & Kanae, S. (2013). Global flood risk under climate change. Nat. Clim. Change, *3*(9), 816-821.

Hirsch, R.M., Archfield, S.A., 2015. Flood trends: Not higher but more often. Nature Clim. Change 5(3), 198-199.

Hoang, L.P., Lauri, H., Kummu, M., Koponen, J., Van Vliet, M.T.H., Supit, I., Leemans, R., Kabat, P., Ludwig, F., 2016. Mekong river flow and hydrological extremes under climate change. Hydrol. Earth Syst. Sc., 20(7), 3027-3041.

Hoang, L.P., van Vliet, M.T. H., Kummu, M., Lauri, H., Koponen, J., Supit, I., Leemans R., Kabat, P., Ludwig, F., 2019. The mekong's future flows under multiple drivers: how climate change, hydropower developments and irrigation expansions drive hydrological changes. Sci. Total Environ. 649, 601-609.

Hossain, F., Sikder, S., Biswas, N., Bonnema, M., Lee, H., Luong, N. D., Long, D., 2017. Predicting water availability of the regulated Mekong river basin using satellite observations and a physical model. Asian J. Water Environ. Pollut. 14(3), 39-48.

Hu, P., Zhang, Q., Shi, P., Chen, B., Fang, J., 2018. Flood-induced mortality across the globe: Spatiotemporal pattern and influencing factors. Sci. Total Environ. 643, 171-182.

Kiem, A. S., Ishidaira, H., Hapuarachchi, H. P., Zhou, M. C., Hirabayashi, Y., & Takeuchi, K. (2008). Future hydroclimatology of the Mekong River basin simulated using the high-resolution Japan Meteorological Agency (JMA) AGCM. *Hydrological Processes: An International Journal*, *22*(9), 1382-1394.

Kummu, M., Lu, X., Wang, J.J., Varis, O., 2010. Basin-wide sediment trapping efficiency of emerging reservoirs along the Mekong. Geomorphology 119(3-4), 181-197.

Kunkel, K.E., Karl, T.R., Brooks, H., Kossin, J., Lawrimore, J.H., Arndt, D., Emanuel, K., 2013. Monitoring and understanding trends in extreme storms: State of knowledge. B. Am. Meteorol. Soc. 94(4), 499-514.

Lauri, H., De Moel, H., Ward, P.J., Räsänen, T.A., Keskinen, M., Kummu, M., 2012. Future changes in Mekong River hydrology: impact of climate change and reservoir operation on discharge. Hydrol. Earth Syst. Sci. Discuss, 9(5), 6569-6614.

Lauri, H., Räsänen, T.A., Kummu, M., 2014. Using reanalysis and remotely sensed temperature and precipitation data for hydrological modeling in monsoon climate: Mekong River case study. J. Hydrometeorol. 15(4), 1532-1545.

Li, F., Chen, D., Tang, Q., Li, W., Zhang, X., 2016. Hydrological response of east China to the variation of East Asian summer monsoon. Adv. Meteorol. 2016, 4038703.

Liang, X., Lettenmaier, D.P., Wood, E.F., Burges, S.J., 1994. A simple hydrologically based model of land surface water and energy fluxes for general circulation models. J. Geophys. Res. Atmos. 99(D7), 14415-14428.

Liang, X., Wood, E.F., Lettenmaier, D.P., 1996. Surface soil moisture parameterization of the VIC-2L model: Evaluation and modification. Global Planet. Change 13(1-4), 195-206.

Liu, J., Zhang, Q., Singh, V. P., Song, C., Zhang, Y., Sun, P., & Gu, X. (2018). Hydrological effects of climate variability and vegetation dynamics on annual fluvial water balance in global large river basins. Hydrology and Earth System Sciences, 22(7), 4047-4060.

Mohammed, I.N., Bolten, J.D., Srinivasan, R., Lakshmi, V., 2018. Satellite observations and modeling to understand the Lower Mekong River Basin streamflow variability. J. Hydrol. 564, 559-573.

MRC, 2006. Annual Flood Report 2005. Mekong River Commission, Vientiane, Lao PDR. 82pp.

MRC, 2007. Annual Mekong Flood Report 2006, Mekong River Commission, Vientiane. 76pp.

MRC, 2009. Annual Mekong Flood Report 2008. Mekong River Commission, Vientiane. 84 pp.

MRC, 2015. Annual Mekong Flood Report 2013. Mekong River Commission. Vientiane, Lao PDR.

Petrow, T., & Merz, B. (2009). Trends in flood magnitude, frequency and seasonality in Germany in the period 1951–2002. J. Hydrol. 371(1-4), 129-141.

Pokhrel, Y., Burbano, M., Roush, J., Kang, H., Sridhar, V., & Hyndman, D. W. (2018). A review of the integrated effects of changing climate, land use, and dams on Mekong river hydrology. Water, *10*(3), 266.

Räsänen, T.A., Kummu, M., 2013. Spatiotemporal influences of ENSO on precipitation and flood pulse in the Mekong River Basin. J. Hydrol. 476, 154-168.

Sheffield, J., Goteti, G., Wood, E.F., 2006. Development of a 50-year high-resolution global dataset of meteorological forcings for land surface modeling. J. Climate 19(13), 3088-3111.

Tang, Q., 2020. Global change hydrology: Terrestrial water cycle and global change. Science China Earth Sciences, 63, 459-462.

Tian, W., Liu, X., Wang, K., Bai, P., Liang, K., & Liu, C. (2021). Evaluation of six precipitation products in the Mekong River Basin. Atmos. Res., 255, 105539.

Triet, N.V.K., Dung, N.V., Hoang, L.P., Duy, N.L., Apel, H., 2020. Future projections of flood dynamics in the vietnamese mekong delta. Sci. Total Environ. 140596.

UNESCO, 2012. Managing water under uncertainty and risk, Facts and Figures from the United Nations World Water Development Report 4 (WWDR4), United Nations World Water Assessment Programme, UNESCO-WWAP.

Wahlstrom, M., Guha-Sapir, D., 2015. The human cost of weather-related disasters 1995–2015. Geneva, Switzerland: UNISDR.

Wang, B., Wu, R., & Lau, K. M. (2001). Interannual variability of the Asian summer monsoon: Contrasts between the Indian and the western North Pacific–East Asian monsoons. *Journal of climate*, *14*(20), 4073-4090.

Wang, W., Lu, H., Yang, D., Sothea, K., Jiao, Y., Gao, B., Pang, Z., 2016. Modelling hydrologic processes in the Mekong River Basin using a distributed model driven by satellite precipitation and rain gauge observations. PloS one, 11(3), e0152229.

Wang, W., Lu, H., Ruby Leung, L., Li, H. Y., Zhao, J., Tian, F., Sothea, K., 2017. Dam Construction in Lancang-Mekong River Basin Could Mitigate Future Flood Risk From Warming-Induced Intensified Rainfall. Geophys Res Lett. 44(20), 10-378.

Wang, Y., Zhang, X., Tang, Q., Mu, M., Zhang, C., Lv, A., Jia, S., 2019. Assessing flood risk in Baiyangdian Lake area in a changing climate using an integrated hydrological-hydrodynamic modelling. Hydrological Sciences Journal, 64(16), 2006-2014.

Wu, H., Adler, R.F., Tian, Y., Huffman, G.J., Li, H., Wang, J., 2014. Real-time global flood estimation using satellite-based precipitation and a coupled land surface and routing model. Water Resour. Res. 50(3), 2693-2717.

Wu, J., Gao, X.J., 2013. A gridded daily observation dataset over China region and comparison with the other datasets (in Chinese with English abstract). China. J. Geophys. 56, 1102–1111.

Yang, R., Zhang, W.K., Gui, S., Tao, Y., Cao, J., 2019. Rainy season precipitation variation in the Mekong River basin and its relationship to the Indian and East Asian summer monsoons. Clim. Dynam. 52(9-10), 5691-5708.

Yatagai, A., Arakawa, O., Kamiguchi, K., Kawamoto, H., Nodzu, M.I., Hamada, A., 2009. A 44-year daily gridded precipitation dataset for Asia based on a dense network of rain gauges. Sola 5, 137-140.

Yatagai, A., Kamiguchi, K., Arakawa, O., Hamada, A., Yasutomi, N., Kitoh, A., 2012. APHRODITE: Constructing a long-term daily gridded precipitation dataset for Asia based on a dense network of rain gauges. B. Am. Meteorol. Soc. 93(9), 1401-1415.

Yun, X., Tang, Q., Wang, J., Liu, X., Zhang, Y., 2020. Impacts of Climate Change and Reservoir Operation on Streamflow and Flood Characteristics in the Lancang-Mekong River Basin. *Journal of Hydrology*, 125472.

Zhang, Q., Gu, X., Singh, V. P., Shi, P., & Sun, P. (2018). More frequent flooding? Changes in flood frequency in the Pearl River basin, China, since 1951 and over the past 1000 years. *Hydrology and Earth System Sciences*, *22*(5), 2637-2653.

Zhao, Q., Ding, Y., Wang, J., Gao, H., Zhang, S., Zhao, C., Shangguan, D., 2019. Projecting climate change impacts on hydrological processes on the Tibetan Plateau with model calibration against the glacier inventory data and observed streamflow. J. Hydrol. 573, 60-81.

Table 1 Detail information for the meteorological and discharge data

Variable	Basin	Dataset	Period	Main source
Precipitation	LRB	CN05.1	1961–2015	Wu and Gao (2013)
	MRB	APHRODITE		*Yatagai et al*. (2009, 2012)
Maximum temperature	LRB	CN05.1		Wu and Gao (2013)
	MRB	Princeton		*Sheffield et al*. (2006)
Minimum temperature	LRB	CN05.1		Wu and Gao (2013)
	MRB	Princeton		*Sheffield et al*. (2006)
Wind speed	LRB	CN05.1		Wu and Gao (2013)
	MRB	Princeton		*Sheffield et al*. (2006)
Discharge	LRB	-	1967–2015	*Henck et al*. (2011)
	MRB	-		*Wang et al*. (2016) *Mohammed et al*. (2018)

* MRB and LRB mean the Mekong River Basin and Lancang River Basin, respectively. The full name of APHRODITE is Asian Precipitation-Highly Resolved Observational Data Integration Toward the Evaluation of Water Resource.

Figure Captions

Figure 1. Overview of the Lancang-Mekong River Basin (LMRB). The 12 hydrological stations from upstream to downstream are Changdou2 (CD2), Jiuzhou (JZ), Gajiu (GJ), Yunjinghong (YJH), Chiang Sean (CS), Luang Prabang (LP), Vien Tiane (VT), Nakhon Phanom (NP), Mukdahan (MD), Pakse (PK), Stung Treng (ST), Kompong Cham (KC), respectively.

Figure 2. Time series of the normalized monsoon indices varying with year from 1967 to 2015. (a), (b), (c) are the normalized Indian Summer Monsoon (ISM), Western North Pacific Monsoon (WNPM), combined monsoon effect (ISWN) indices, respectively.

Figure 3. The basic flowchart of the monsoon impact on flood

Figure 4. Spatial distributions of rainfall anomalies in the weak monsoon (L; bottom) and strong monsoon (H; top) years. The panels from left to right denote ISM, WNPM, and ISWN, respectively. The dashed polygon in the top panel represents the monsoon impact area.

Figure 5. Comparisons of flood characteristics extracted from both the observed and simulated discharges at three representative stations. Onset, termination also refer to the start date and end date, respectively.

Figure 6. The flood characteristic anomalies at three representative stations during the strong and weak monsoon years. The signs O, T, D, P, V, Q separately refer to the Onset (start date), Termination (end date), duration, peak, volume, and Q_{10} for the convenience of drawing the figures. L means the weak monsoon, H means the strong

monsoon.

Figure 7. The distributions of the simulated flood characteristic anomaly in the weak ISM (L) and strong ISM (H) years. The numbers in each subfigure show the average change, and area percent of monsoon impact area having the average change, respectively. For example, (a) indicates over 65.4% of the monsoon impact area averagely changes the flood start date by -4.4%.

Figure 8. The distributions of the simulated flood characteristic anomaly in the strong (H) and weak (L) WNPM years. Other signals are similar with Figure 7.

Figure 9. The distributions of the simulated flood characteristic anomaly in the strong (H) and weak (L) ISWN years. The signals see Figure 7.

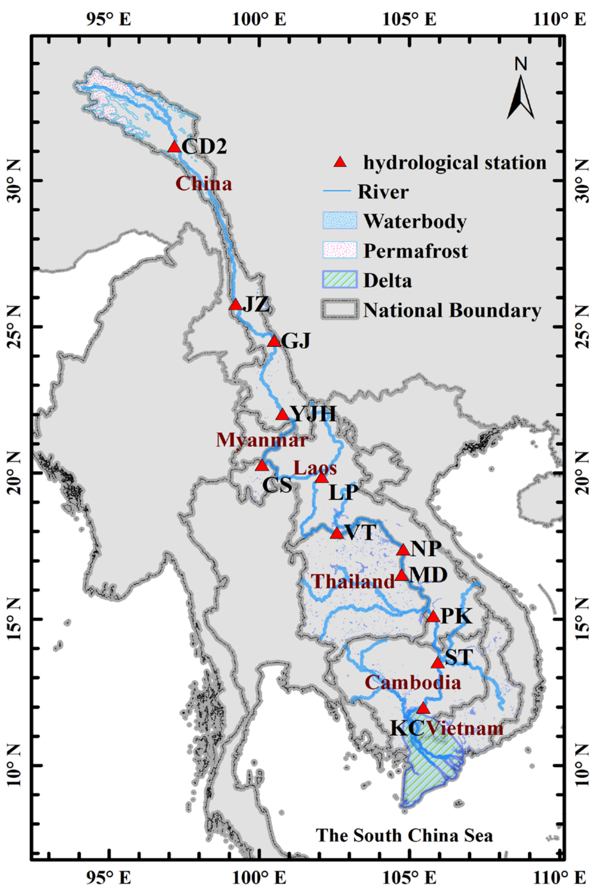

Figure 1. Overview of the Lancang-Mekong River Basin (LMRB). The 12 hydrological stations from upstream to downstream are Changdou2 (CD2), Jiuzhou (JZ), Gajiu (GJ), Yunjinghong (YJH), Chiang Sean (CS), Luang Prabang (LP), Vien Tiane (VT), Nakhon Phanom (NP), Mukdahan (MD), Pakse (PK), Stung Treng (ST), Kompong Cham (KC), respectively.

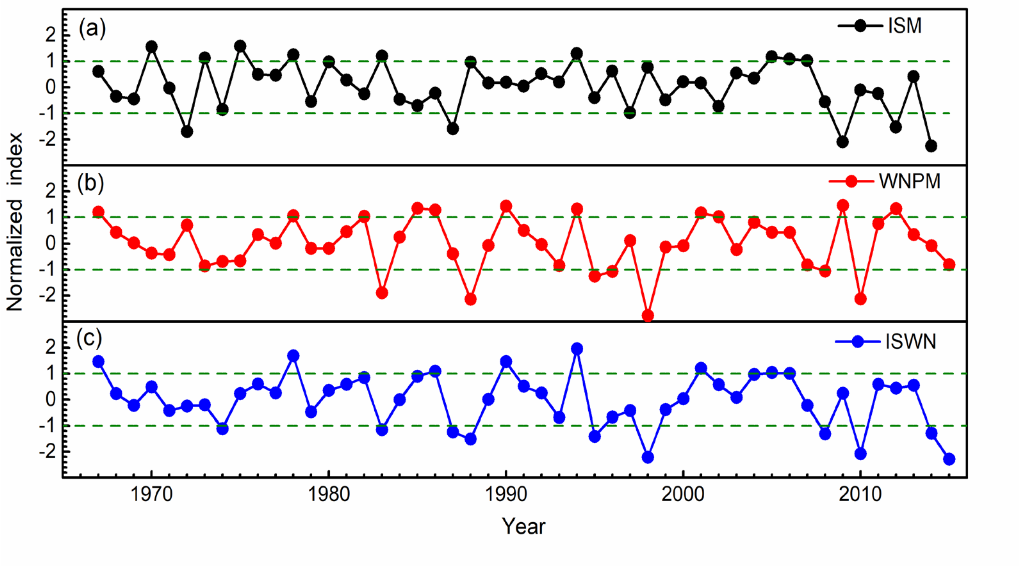

Figure 2. Time series of the normalized monsoon indices varying with year from 1967 to 2015. (a), (b), (c) are the normalized Indian Summer Monsoon (ISM), Western North Pacific Monsoon (WNPM), combined monsoon effect (ISWN) indices, respectively.

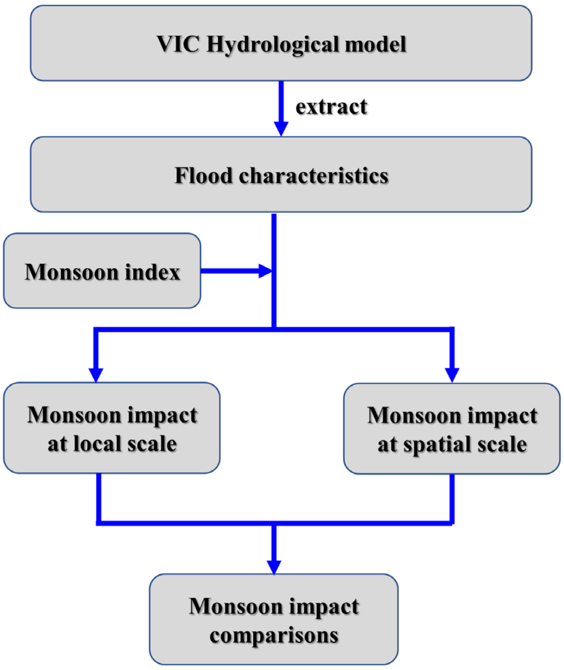

Figure 3. The basic flowchart of the monsoon impact on flood

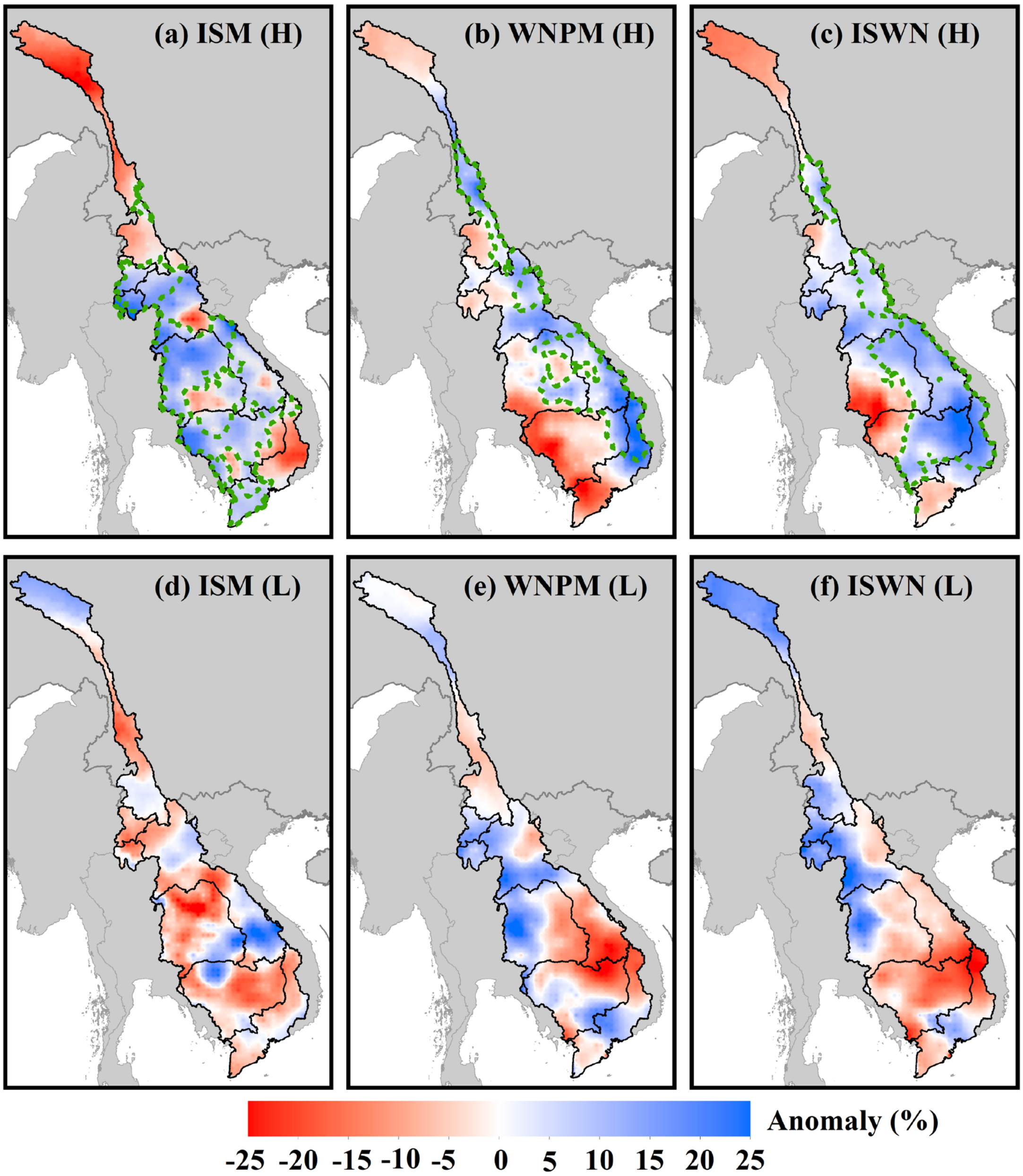

Figure 4. Spatial distributions of rainfall anomalies in the weak monsoon (L; bottom) and strong monsoon (H; top) years. The panels from left to right denote ISM, WNPM, and ISWN, respectively. The dashed polygon in the top panel represents the monsoon impact area.

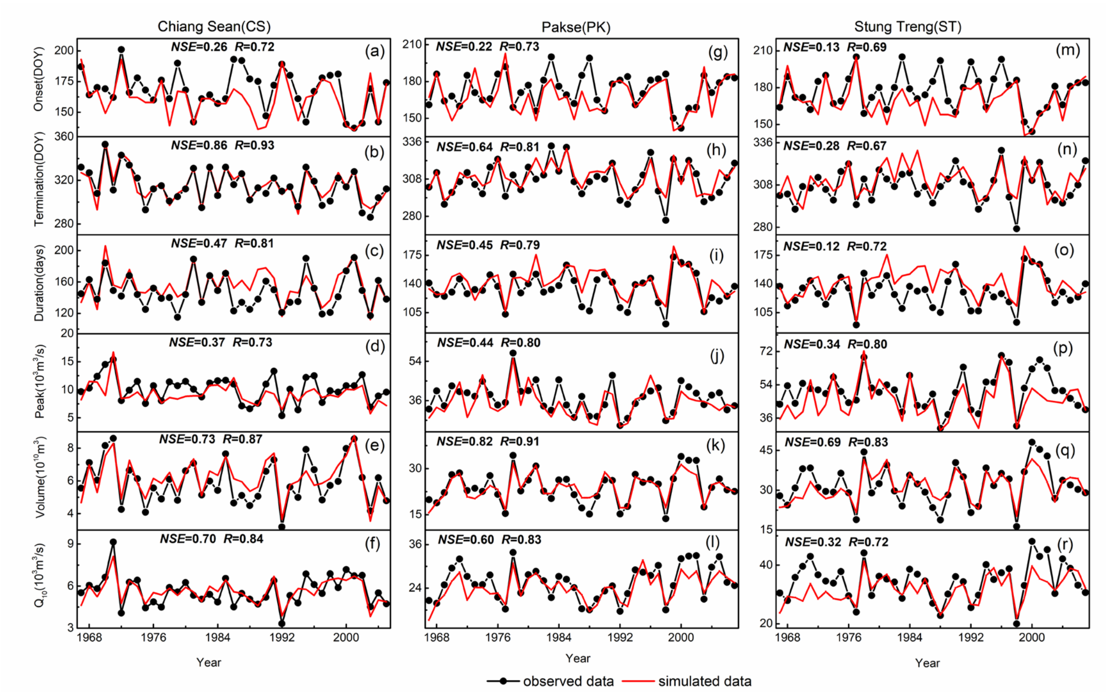

Figure 5. Comparisons of flood characteristics extracted from both the observed and simulated discharges at three representative stations. Onset, termination also refer to the start date and end date, respectively.

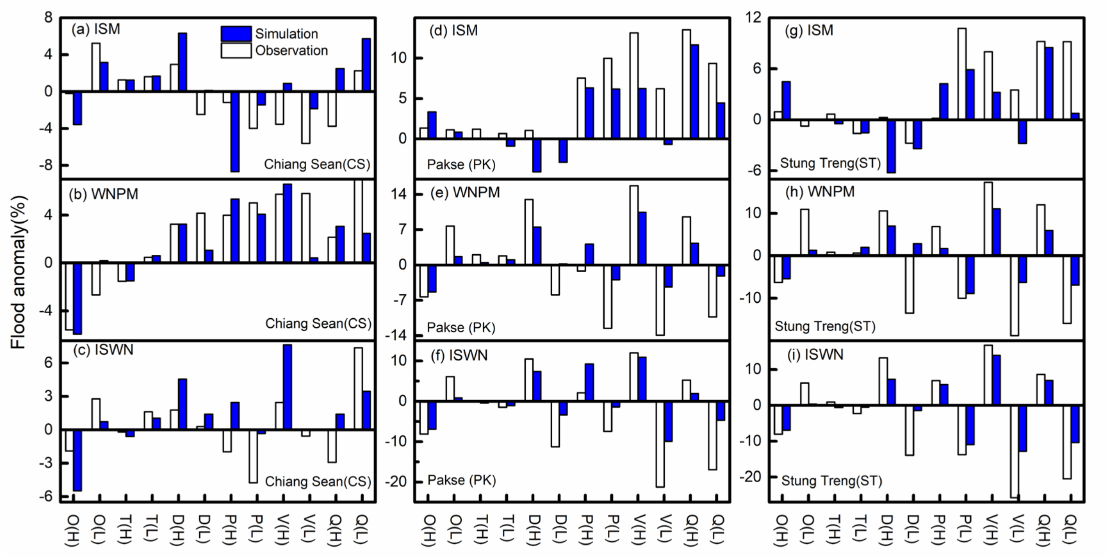

Figure 6. The flood characteristic anomalies at three representative stations during the strong and weak monsoon years. The signs *O*, *T*, *D*, *P*, *V*, *Q* separately refer to the Onset (start date), Termination (end date), duration, peak, volume and Q_{10} for the convenience of drawing the figures. L means the weak monsoon, H means the strong monsoon.

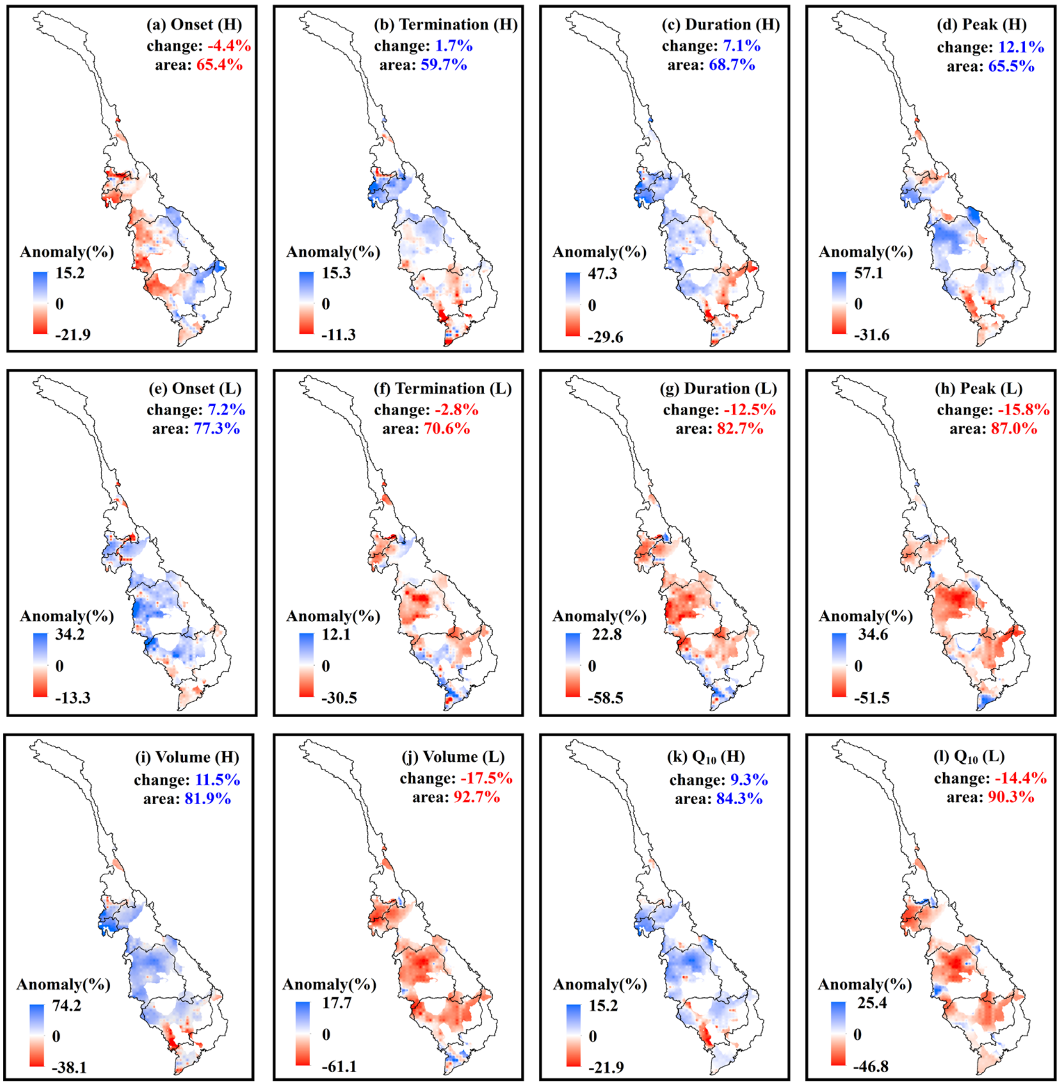

Figure 7. The distributions of the simulated flood characteristic anomaly in the weak ISM (L) and strong ISM (H) years. The numbers in each subfigure show the average change, and area percent of monsoon impact area having the average change, respectively. For example, (a) indicates over 65.4% of the monsoon impact area averagely changes the flood start date by -4.4%.

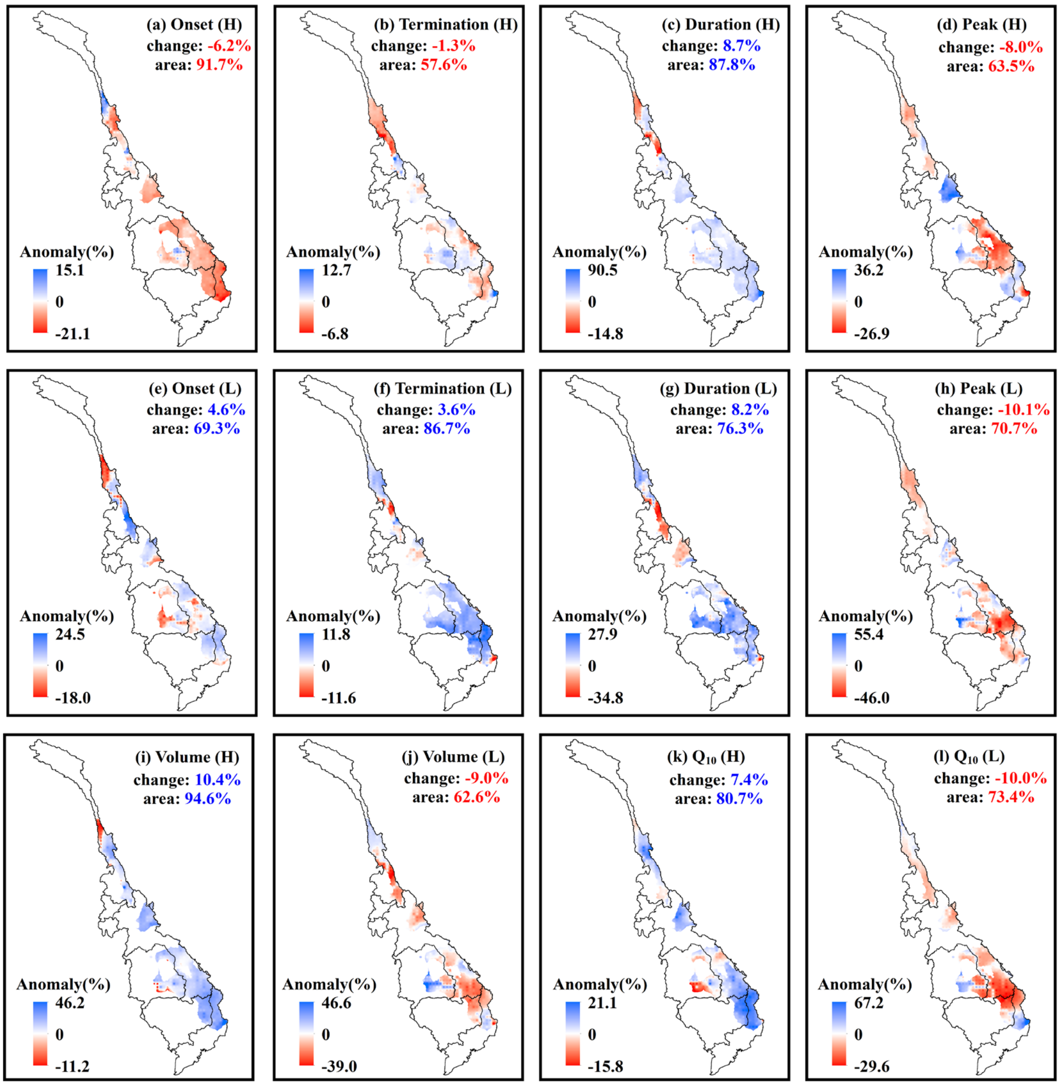

Figure 8. The distributions of the simulated flood characteristic anomaly in the strong (H) and weak(L) WNPM years. Other signals are similar with Figure 7.

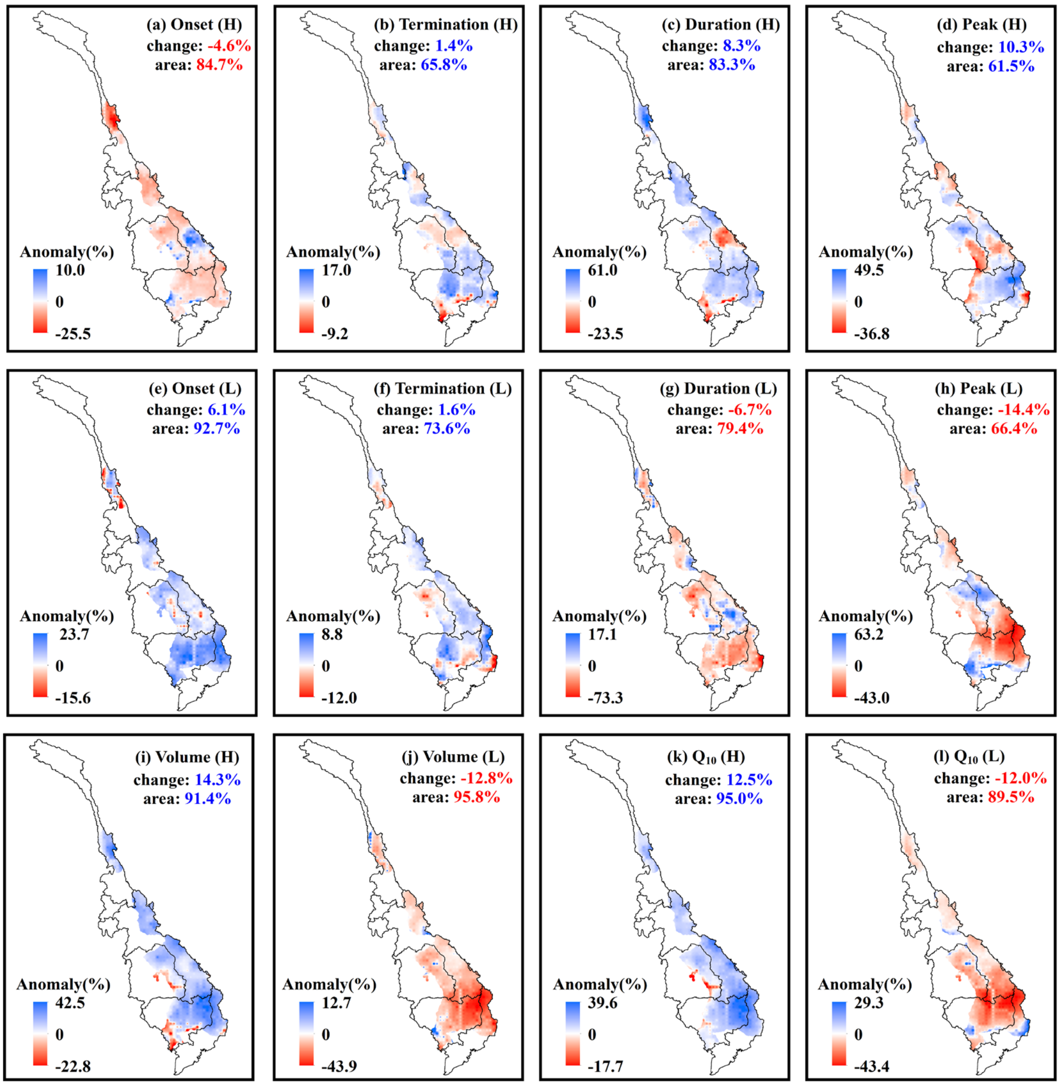

Figure 9. The distributions of the simulated flood characteristic anomaly in the strong (H) and weak (L) ISWN years. The signals see Figure 7.